Stabilization Mechanisms of Retained Austenite in Transformation-Induced Plasticity Steel

JIAJUN WANG and SYBRAND VAN DER ZWAAG

Three stabilization mechanisms—the shortage of nuclei, the partitioning of alloying elements, and the fine grain size—of the remaining metastable austenite in transformation-induced plasticity (TRIP) steels have been studied by choosing a model alloy Fe-0.2C-1.5Mn-1.5Si. An examination of the nucleus density required for an athermal nucleation mechanism indicates that such a mechanism needs a nucleus density as large as $2.5 \cdot 10^{17}$ m^{-3} when the dispersed austenite grain size is down to 1 μm. Whether the random nucleation on various heterogeneities is likely to dominate the reaction kinetics depends on the heterogeneous embryo density. Chemical stabilization due to the enrichment of carbon in the retained austenite is the most important operational mechanism for the austenite retention. Based on the analysis of 57 engineering steels and some systematic experimental results, an exponential equation describing the influence of carbon concentration on the martensite start (M_s) temperature has been determined to be M_s (K) = 273 + 545.8 $\cdot$ $e^{-1.362 w_C (\text{mass pct})}$. A function describing the M_s temperature and the energy change of the system has been found, which has been used to study the influence of the grain size on the M_s temperature. The decrease in the grain size of the dispersed residual austenite gives rise to a significant decrease in the M_s temperature when the grain size is as small as 0.1 μm. It is concluded that the influence of the grain size of the retained austenite can become an important factor in decreasing the M_s temperature with respect to the TRIP steels.

I. INTRODUCTION

VARIOUS phase transformations, *i.e.*, proeutectoid ferrite,[1] bainite,[2] martensite,[3] and intermetallic precipitation reactions,[4,5] may take place in a steel grade exhibiting transformation toughening.[6] The occurrence of a specific phase transformation depends on the alloy composition and heat-treatment procedures,[7,8] while the amount of retained austenite at room temperature in such a steel grade depends largely on the martensite start (M_s) temperature of the dispersed austenite with a very small grain size. It is known that most engineering steels, after regular austenitizing, have an average austenite grain size ranging from 20 to 100 μm. On such a size scale, the influence of the grain size on the M_s temperature is negligible, which is in contrast to that on the premartensitic reactions, such as the proeutectoid ferrite, pearlite, and bainite reactions. Results reported by Kajiwara *et al.*[9] suggested that ultrafine austenite particles (20 to 200 nm) transformed at the same M_s temperature as that for the corresponding bulk alloy. On the other hand, it was reported that the M_s temperature might rise by approximately 40 K when the austenitization temperature is raised from 1073 to 1473 K.[10,11] However, the use of this fact to support the significance of the grain-size effect is arguable, because it is difficult to disentangle the effect of changing austenite grain size from those of a changing defect structure, the homogeneity of the solid solution, and segregation.[12] Investigation of the decomposition of small austenite particles shows that the kinetics of isothermally formed martensite depends largely on the grain size when it is down to 20 μm.[12,13] Fine-grained austenite generally has a relatively low M_s temperature or high stability during either thermal or mechanical processing.[14,15] Fisher *et al.*[16] modeled the influence of austenite grain size on the extent of martensite transformation and concluded that a decrease in grain diameter lowers the experimental M_s temperature. Obviously, the influence of grain size on the martensitic reaction in steel remains unclear. With respect to the steels demonstrating a transformation-induced plasticity (TRIP) effect,[6,15] the question seems more important, because the average dispersed austenite grain size in question is between 0.1 and 20 μm[17] due to the partitioning of the matrix by large portions of ferrite and bainite transformation products. The dimension of the dispersed austenite trapped inside bainitic ferrite sheaves may well be smaller than 0.1 μm. If the Fisher–Hollomon diminishing-size effect[16] is also considered, the size span of retained austenite can be down to an atomic scale. The transformation behavior involved may resemble that in the Fe-based nanocrystals.[18] Clearly, from either the engineering or the fundamental point of view, examining the stabilization mechanism of small austenite particles is of great importance.

II. METHODOLOGY

In this article, the compositions of the residual austenite after a proeutectoid ferrite reaction under both local equilibrium[19] and paraequilibrium[20] conditions will be determined based on a series of thermodynamic calculations.[21] Meanwhile, an analytical method will be introduced to calculate the carbon concentration of the residual austenite after both the ferrite and bainite reactions, without invoking the expensive and complicated thermodynamic software when a paraequilibrium assumption has been made. The changes in the average grain size of the dispersed metastable austenite

JIAJUN WANG, Researcher and Metallurgist, formerly with the Netherlands Institute for Metals Research, Rotterdamseweg 137, 2628 AL Delft, is with Philips Lighting B.V., 6026RX Maarheeze, The Netherlands. SYBRAND VAN DER ZWAAG, Professor, is with the Department of Materials Science, Delft University of Technology, Rotterdamseweg 137, 2628 AL Delft, The Netherlands.

Manuscript submitted May 16, 2000.

due to both the ferrite and bainite reactions were estimated by a geometric model.[22] Three possible mechanisms[23] that may be responsible for the austenite retention have been discussed: the shortage of nuclei, chemical stabilization, and the grain-size effect. The discussion on the shortage of nuclei is mainly based on the assumption that martensitic decomposition is an athermal process determined by the pre-existing nucleus density.[24] The chemical stabilization arises from the partitioning of alloying elements during both the ferrite and bainite reactions. The influence of the composition of the dispersed austenite on its M_s temperature has been expressed by a statistical equation based on our previous results.[25] Finally, the energy-balancing method[21] has been used to model the effect of the austenite grain size on the stabilization by considering the change of the total system energy, in which the influence of the chemistry and temperature on the elastic moduli and lattice parameters of ferrite, austenite, and martensite has been considered.

III. THERMODYNAMIC CALCULATIONS ON TRIP STEELS

A. *Phase Diagrams*

An Mn-Si–containing TRIP steel (Fe-0.16C-1.5Mn-1.5Si) has been taken as an example throughout this article, although most of the calculations and the discussion made hereafter can be easily applied to any other alloys. Thermal heat treatments imposed resemble those used in producing real TRIP steels, including the intercritical annealing and austempering.[22] The vertical section of the quaternary diagram of Fe-C-1.5Mn-1.5Si is calculated and shown in Figure 1(a) by assuming a local equilibrium, in which all alloying elements are capable of partitioning inside and amongst the three phases present (austenite, ferrite, and cementite). All thermodynamic calculations were done by a commercial software package, MTData,[26] based on the Scientific Group Thermodata Europe (SGTE). Note that, in most cases, we wrote special macro functions for MTData, which give us the flexibility to handle the complicated equilibrium conditions.

Clearly, the A_1 temperature (not exactly A_1, since Figure 1 is only a quasi diagram) has split over a range between 970 and 984 K. The A_3 temperature is approximately 1137 K. Providing that the intercritical annealing temperature is between 973 and 1133 K, a certain volume of ferrite remains (upon heating) or precipitates (upon cooling). In practice, since the intercritical annealing time is normally very short, it is reasonable to assume that cementite does not precipitate and the partitioning of substitutional alloying elements (Mn and Si) cannot be fulfilled within the intercritical temperature range. With these assumptions taken into consideration, the vertical section of the quaternary diagram is recalculated and given in Figure 1(b). It should be kept in mind that the phase boundaries illustrated in Figure 1 cannot be used to determine the carbon equilibrium concentration at different temperatures because of the partitioning of substitutional alloying elements.

B. *Carbon Concentration of Residual Austenite*

One of the most important heat-treatment procedures for TRIP steels is the intercritical annealing, during which nearly carbon–free ferrite and carbon-enriched austenite form,

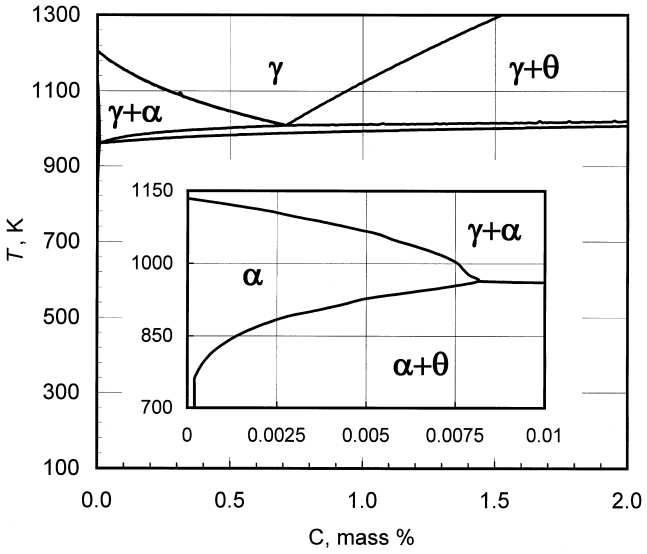

(*a*)

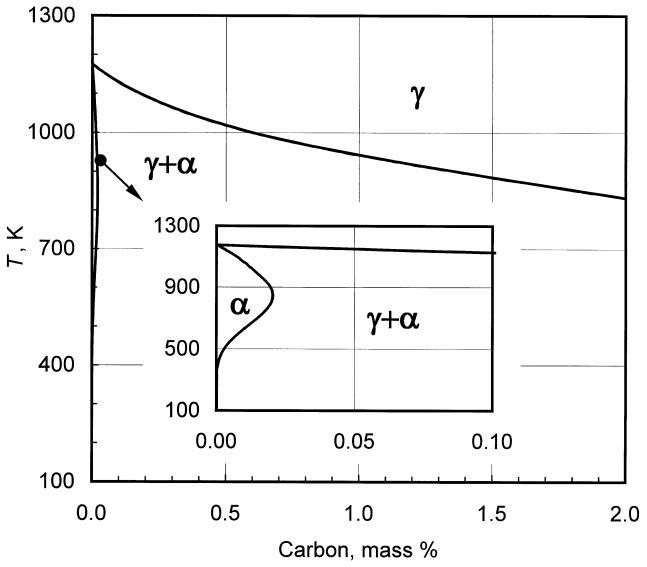

(*b*)

Fig. 1—Thermodynamic calculation of the cross-sectional phase diagram of an Fe-C-1.5Mn-1.5Si system by assuming (*a*) full equilibrium among three phases γ (austenite), α (ferrite), and θ (cementite) and partitioning of all alloying elements, and (*b*) equilibrium between γ and α, and partitioning of carbon, without the precipitation of θ and partitioning of Mn and Si.

since the ferrite and bainite decompositions[27] are accompanied by the redistribution of (at least) interstitial atoms. Therefore, the carbon concentration of the retaining austenite is certainly different from that of the nominal concentration and is dependent on the volume fraction of the ferrite present. In this subsection, two methods will be explained to calculate the carbon concentration of residual austenite after the ferrite or bainite reactions: thermodynamic methods and analytical ones. With respect to the thermodynamic methods, two different equilibrium conditions will be considered hereafter: local equilibrium and paraequilibrium. For each equilibrium condition, we can also define the number and type of phases that may appear in the system.

Figure 2(a) shows the thermodynamically calculated

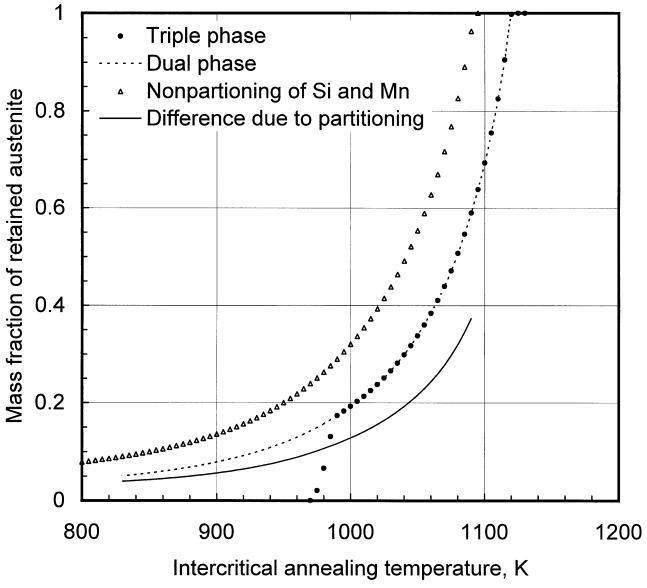

(*a*)

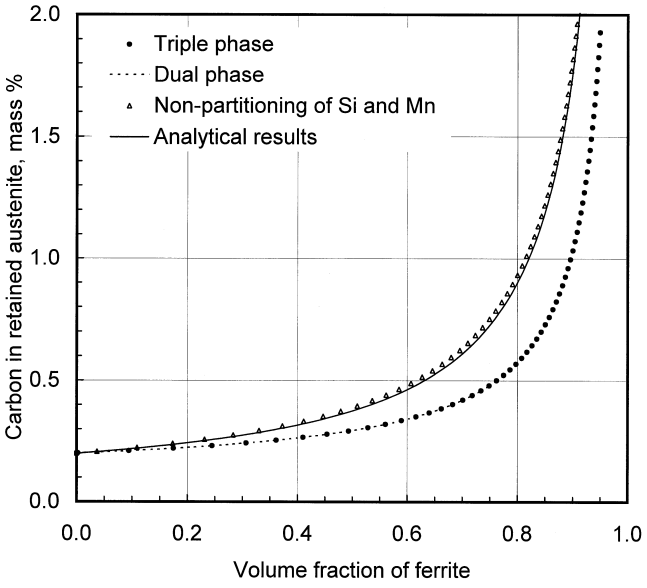

(*b*)

Fig. 2—Mass fraction and carbon concentration of retained austenite in the Fe-0.2C-1.5Mn-1.5Si TRIP steel. (*a*) Mass fraction of retained austenite as a function of the intercritical annealing temperature. Triple-phase curve: three phases γ, α, and θ present and all alloying elements partitioned; dual-phase curve: two phases γ and α present and all alloying elements partitioned; and nonpartitioning of Si and Mn: two-phase (γ and α) equilibrium without the partitioning of Si and Mn. (b) Carbon concentration as a function of the volume fraction of ferrite; the assumptions are the same as those for the curves, respectively, in (a); the other curve is the result calculated from Eq. [3].

results on the mass fraction of residual austenite after being intercritically annealed at different temperatures. If all alloying elements are allowed to redistribute, the amount of retained austenite calculated at the temperature range between 1000 and 1100 K by assuming either triple-phase or dual-phase equilibrium is the same. This is because within this temperature range, neither the alloy carbide nor cementite precipitates. However, if the partitioning of Si and Mn is not allowed, or the system is under paraequilibrium, the mass fraction of the retained austenite increases, as shown by the shift in Figure 2(a). The difference between the two curves, shown by the solid line in Figure 2(a), can be up to 0.4. Therefore, care should be taken when using the thermodynamic model to estimate the amount of retained austenite after intercritical annealing, since full partitioning of all alloying elements is the default assumption and is widely used in some thermodynamic software packages. Practically, the equilibrium must be reached somewhere between the first two top curves in Figure 2(a). As has been discussed elsewhere,[22] the partitioning of substitutional alloying elements is highly possible during the intercritical annealing. However, for simplicity, we use the nonpartitioning results to approximate the equilibrium situation in this article.

In addition to the mass fraction of retained austenite, the carbon concentration in the metastable austenite can be calculated by the thermodynamic method. The curves in Figure 2(b) shows the carbon concentration of the remaining austenite, which clearly depends on the volume fraction of ferrite. The latter depends on the intercritical annealing temperature. The calculations in Figure 2(b) are based on the same equilibrium assumptions as those used to calculate Figure 2(a). The difference between the two carbon concentrations, arising from different equilibria assumptions imposed on Si and Mn, is very clear. This further indicates that the partitioning of Si and Mn attending this system is very important and, thus, deserves further investigation.

As is illustrated previously, the thermodynamic calculation requires a basic knowledge of equilibrium conditions, the choice of a thermodynamic database, and the use of a dedicated software package to determine the multiphase equilibria. Therefore, it is not convenient for engineers to use this method to calculate the carbon concentration in the residual austenite. In fact, the carbon concentration can be analytically expressed by the following equation (refer to the Appendix for derivative details):

$$x_\gamma = \left[1 + \frac{X_B V_B^m + X_F V_F^m}{\dfrac{x_\gamma^0}{1 - x_\gamma^0} - \dfrac{X_B x_B}{1 - x_B} - \dfrac{X_F x_F}{1 - x_F}} \frac{f_\gamma}{V_\gamma^m (1 - f_\gamma)} \right]^{-1} \quad [1]$$

where X_P represents the mole fraction of different phases, denoted by P. In our case, P is either ferrite, bainite, or remaining austenite, while the indices of B and F represent bainite and ferrite, respectively. The term x_γ^0, called the mole atom fraction (which is different from the mole lattice-site fraction) is the average carbon concentration of the mass alloy; x_P represents the carbon mole fractions of the corresponding phases; f_P represents the volume fractions of different phases; and V_P^m represents the molar volumes of austenite and ferrite. Note that two types of molar volumes of phases have been used in this article: the molar atom volume (V_P^m) and the molar lattice-site volume (V_m^P), which appears in Eq. [4] in this article. Let us take austenite as an example to examine the difference between the two molar volumes. The term V_γ^m is defined as the volume of 1 mole of atom, which includes both substitutional (Fe, Mn, Si, . . .) and interstitial atoms (C, N, or B). However, V_m^γ refers to the volume of 1-mole sites of the fcc lattice, in which the interstitial atoms (C, N, or B) are not considered based on the assumption that all lattice sites are occupied by substitutional alloying atoms only. The term V_m^γ is a function of the lattice

parameter, while V_γ^m depends on both the lattice parameters and carbon concentrations. Apparently, for a substitutional solid solution, the use of V_P^m and V_m^P make no difference. In the case of TRIP steel, if the composition of the residual austenite is Fe-2.0C-1.5Mn-1.5Si, $V_\gamma^m = (1 - 0.085431)V_m^\gamma$. The difference is very clear.

If the carbon concentrations of bainite and ferrite are assumed to be the same and are taken to be the equilibrium carbon concentration, as that in the ferrite, then the only parameter needed to solve Eq. [1] is either X_B or X_F. From Figure 1, it is clear that it is safe to take the equilibrium carbon concentration in ferrite as 0.02 mass pct (approximately 0.001 in mole fraction). If the following additional approximations are made,

$$\begin{cases} V_B^m = V_F^m = V_\gamma^m = V_m \\ x_B = x_F = 0.001 \end{cases} \quad [2]$$

then Eq. [1] is reduced to

$$x_\gamma = \left[1 + \frac{f_\gamma}{\dfrac{x_\gamma^0}{1 - x_\gamma^0} - (1 - f_\gamma) \cdot 10^{-3}} \right]^{-1} \quad [3]$$

That is, the carbon concentration of the remaining austenite depends only on the volume fraction of the metastable austenite in a given alloy. The calculated results from Eq. [3] are given in Figure 2(b), which shows the dependency of the carbon concentration on the volume fraction of ferrite in the Fe-0.2C-1.5Mn-1.5Si (mass pct) steel and is approximately equal to the mass fraction under the conditions given in Eq. [2]. It is clear that Eq. [3] is sufficiently accurate to approximate the results calculated from the complex thermodynamic model. From the procedures used to derive Eq. [3], it is clear that Eq. [3] can also be applied to other TRIP steels, *e.g.*, Fe-C-Mn-*X* (*X* = Al, P, Si, or a mixture of some of these).

Note that, in addition to the assumptions given in Eq. [2], Eq. [3] holds only when

(1) All pearlite colonies are fully dissolved during intercritical annealing, or no pearlitic cementite exists after intercritical annealing.
(2) Neither alloy carbide nor cementite precipitates in either austenite (proeutectoid type) or ferrite (interphase type). In an isolated case, carbide formation has been observed in the proeutectoid ferrite in the P-containing TRIP alloys.[28] However, the amount of the precipitation is too small to exert much influence.
(3) No pearlite reaction occurs during cooling from the intercritical annealing temperature to the isothermal temperature.
(4) No bainitic carbide appears in the bainitic ferrite sheaves, due to the higher Si content.[29,30] In the case of TRIP steels, the assumptions for deriving Eq. [3] are reasonable, and, thus, the equation obtained should be applicable. In practice, the volume fraction of residual austenite is around 0.10 to 0.20. The corresponding carbon concentration can be easily estimated from Figure 2(b) in the range from 0.9 to 2.0 mass pct. Thus, most of the discussion henceforward will be focused on the alloys with a carbon concentration range between 1.0 and 2.0 mass pct.

IV. SPATIAL GEOMETRICAL DESCRIPTION OF A FINE GRAIN SYSTEM

Austenite grains tends to be closely packed and in the shape of polyhedrons.[31] A polyhedron can be approximately regarded as a globe at an equivalent diameter of d_0. One mole of austenite contains n_0^γ grains of a diameter of d_0, where

$$n_0^\gamma \approx \frac{6V_m^\gamma}{\pi d_0^3} \quad [4]$$

where V_m^γ is the molar lattice-site volume of austenite. The first few martensitic plates span the austenite grains. The diameter of such martensite plates is determined by the austenite grain size, d_0. The surface area of such a martensitic plate formed near the center of an austenite grain is approximately given by

$$A_0^{\alpha'} \simeq 2\pi \left(\frac{d_0}{2} \right)^2 \simeq \frac{\pi d_0^2}{2} \quad [5]$$

in which the surface area of the plate edges is neglected. If the aspect ratio of a martensite plate is defined as

$$\iota = \frac{\delta}{d_0} \quad [6]$$

where δ denotes the thickness of the plate, the number of plates constituting 1 mole of martensite is

$$n_m^{\alpha'} = \frac{V_m^{\alpha'}}{V_0^{\alpha'}} = \frac{4V_m^{\alpha'}}{\pi \delta d_0^2} = \frac{4V_m^{\alpha'}}{\pi \iota d_0^3} \quad [7]$$

where the molar lattice-site volume of the martensite is represented by $V_m^{\alpha'}$. The influence of the carbon concentration on the lattice parameter of the martensitic ferrite has been considered in this article. A program has been made to calculate the lattice parameters of martensite, a and c.[32] The molar volume of martensite is then derived by calculating the volume of the unit cell.

We now define the M_s temperature at which a 1 pct volume of martensite is formed. Accordingly, the mole number of austenite required to form 1 mole of martensite ($N_\alpha = 1$) at the M_s temperature is written as

$$N_\gamma = \frac{99V_m^{\alpha'} N_{\alpha'} + V_m^\gamma}{V_m^\gamma} = \frac{99V_m^{\alpha'} + V_m^\gamma}{V_m^\gamma} \quad [8]$$

Note that the total austenite mole number required does not equal 100 moles, because of the difference between the molar lattice-site volumes of ferrite and austenite. A similar difference exists also with respect to the molar atom volumes, but has been ignored in Eq. [2].

Multiplication of N_γ by n_γ^0 generates the number of austenite grains required to form 1 mole of martensite, that is,

$$n^\gamma = N^\gamma n_0^\gamma = \frac{99V_m^\alpha + V_m^\gamma}{\pi d_0^3/6} \quad [9]$$

V. POTENTIAL OPERATIONAL MECHANISMS FOR STABILIZATION

It should be noted that some empirical models have been well established[33,34] to account for the influence of the austenite grain size on the yield strength of a steel, but

these theories are by no means helpful for the understanding of the effect of the austenite grain size on the martensitic transformation, in spite of the analogy of the martensite transformation to plastic deformation. Various alternative mechanisms for the stabilization of retained austenite and their relation to the austenite grain size will be henceforth discussed.

A. *Shortage of Heterogeneous Nuclei*

Nowadays, arguments still exist as to whether the martensite nucleation reaction is an athermal[14,35] or thermal[9,36] process. In an athermal process, prior to the reaction, the martensite nuclei are supposed to exist in the parent phase. This idea is strongly supported by a small-droplet experiment.[14] A thermal process means that the martensite nucleation is thermally activated. We first assume that the martensitic reaction is an athermal process without the help of thermal activation.

For the modeling of TRIP (Fe-0.2C-1.5Mn-1.5Si) steels at room temperature (298 K), the carbon concentration in the retained austenite having experienced ferrite and bainite decompositions is taken to be 1.6 mass pct (the amount of retained austenite is about 13 vol pct), as shown in Figure 2(b). The molar lattice-site volumes of austenite and martensite are calculated to be 7.217 and $7.425 \cdot 10^{-6}$ m^3/mole at room temperature; then,

$$\frac{n^{\gamma}}{n_m^{\alpha'}} = \frac{3(99 + V_m^{\gamma}/V_m^{\alpha'})}{2}\,\iota \simeq 150\iota \qquad [10]$$

Thus, if $\iota < 1/150$, $n^{\gamma} < n_m^{\alpha'}$. This means that a certain number of austenite grains must contain more than one martensite plate. The aspect ratio of the martensite plate was reported to be within 1/15 to 1/30,[12] with an average of 0.05 in high-carbon steels.[37] Meanwhile, it has also been reported[38–42] that the aspect ratio of the martensite varies with the alloy composition, formation temperature, and volume fraction of the martensite formed. The work done on a high-carbon low-alloy steel[43,44] has proven that the aspect ratio of the martensite increases with the increase in the volume fraction of the martensite formed. However, the experimental data in these reports also showed that the change of the aspect ratio is less than 4 pct when the volume fraction of martensite increases from 0 to 0.01. Therefore, as a reasonable approximation, we set the constant value of 0.05 for the aspect ratio, and, thus, $n^{\gamma} > n_m^{\alpha}$. This indicates that the martensite transformation does not occur in every austenite grain at the M_s temperature. It should be pointed out that the influence of the aspect ratio will be further discussed in Figure 7.

Figure 3 shows the number of austenite grains (Eq. [9]) and martensite plates (Eq. [7]) involved in the formation of a 1 pct volume of martensite at the M_s temperature. The solid line represents the number of austenite grains. Three dotted lines correspond to the numbers of martensite plates having specific aspect ratios. As is clearly shown in Figure 3 and Eq. [10], the number of austenite grains required depends significantly on the aspect ratio of the martensite plate. If the aspect ratio is taken to be 0.01, the numbers required and present are roughly of the same order of magnitude. At an aspect ratio of 0.1, the number of austenite grains required is only 1/15 of that present. Note that the ratio of

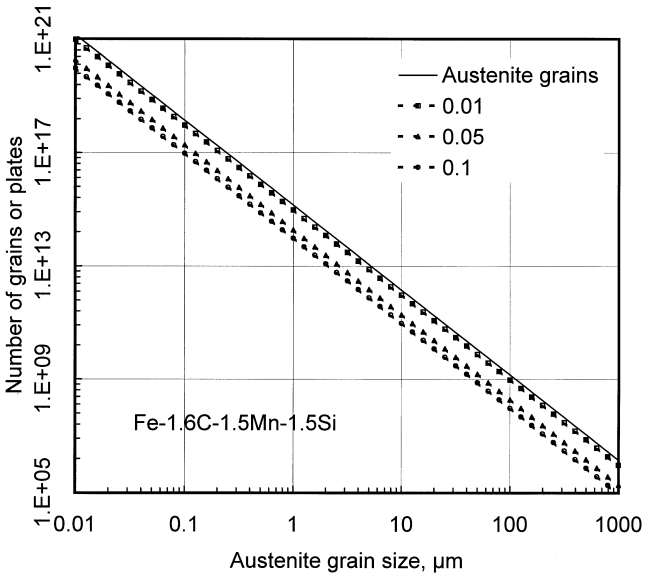

Fig. 3—Number of austenite grains and martensite plates associated with the formation of 1 mole martensite at the M_s temperature (1 vol pct); different dashed lines correspond to different aspect ratios.

Eq. [10] is barely affected by the austenite grain size. This implies that even for engineering steels, the aspect ratio of the martensite plates could not be smaller than 0.01; otherwise, the heterogeneous nucleation mechanism should be excluded.

As mentioned previously, the aspect ratio of the martensite plate is reported to be 0.05;[37] thus, the number of austenite grains available is 7 times larger than the number of martensite plates. This implies that, geometrically, it is possible for all martensite plates to form in different austenite grains, as long as heterogeneous nuclei are available throughout the parent phase. It is, therefore, worthwhile to check if sufficient nuclei are available.

The prerequisite for the athermal nucleation is the preexistence of a certain number of nuclei.[45] It is clear that the smaller the size of the martensite plates, the larger the number of nuclei needed in case burst transformation does not take place. If the thermal activation condition for nucleating is not satisfied, the lack of heterogeneous nuclei will give rise to the absence of the martensitic reaction, or stabilization of the retained austenite. This is similar to the droplet experiment done by Turnbull and Vonnegut,[46] where subdividing the system into more droplets made most droplets to be free from potent heterogeneous nuclei.

Figure 3 shows clearly that the decrease in austenite grain size gives rise to an increase in the number of nuclei required to form a 1 pct volume of martensite plates. If the initial nuclei are uniformly distributed throughout the austenite and not associated with grain boundaries,[13] the number of nuclei in a small grain is proportional to its volume.[47] The density of nuclei is taken to be $\rho_N = 10^7$ cm^{-3} $= 10^{13}$ m^{-3}, based on the transformation behavior of small particles.[14] The average number of nuclei in one austenite grain can be calculated:

$$n_m^N = \rho_N V_0^{\gamma} = \frac{\pi d_0^3}{6}\,\rho_N \qquad [11]$$

If the nucleation of martensite consumes the potent nuclei,

the maximum number of plates needed to form 1 mole of martensite should be no more than the potent nuclei existing in the matrix. Mathematically, this is written as

$$n_m^{\alpha'} \leq n_m^N n^\gamma \qquad [12]$$

It can be argued that the well-known autocatalytic effect may introduce more nuclei during the formation of martensite. However, it was reported that the martensite reaction in carbon and low-alloy steels is athermal rather than a burst (autocatalytic) type.[12] Basically, there are three types of autocatalytic nucleation mechanisms: face-to-face, edge-to-face, and edge-to-edge.[48] As far as the martensite reaction is concerned, the face-to-face mechanism may apply to lath martensite, which is certainly beyond the scope of this article, since the carbon concentration involved is higher than 1.0 mass pct. The edge-to-edge mechanism may be responsible for the burst martensitic reaction in the Fe-Ni-C alloys. Although it was also reported that the burst transformation might take place in the carbon steels when the carbon concentration is higher than 1.4 mass pct, the kinetics measurements are not convincing. In this article, we will not consider the autocatalytic phenomenon.

Substituting for the relative expressions in the previous equation, we obtain the expression for the critical grain size:

$$d_0^{\min} \geq \left(\frac{4}{\pi \iota \rho_N (99 + V_m^\gamma / V_m^{\alpha'})} \right)^{1/3} \qquad [13]$$

Figure 4(a) shows the critical grain size required to form 1 mole of martensite for three given nucleus densities. The carbon concentration is taken to be 1.6 mass pct. If the nucleus density is 10^{13} m^{-3}, $d_0^{\min}$ decreases with increasing aspect ratio, as shown in Figure 4(a). At an aspect ratio of $\iota = 0.05$, the value of $d_0^{\min}$ is about 29.4 μm. This indicates that, according to Eq. [13], the volume fraction of martensite cannot exceed a 1 pct volume if the austenite grain size is smaller than about 30 μm, unless the nucleus density is increased. In other words, it is difficult to detect experimentally the M_s temperature, since the amount formed is too small. Note that the effect of the grain size described in Eq. [13] is actually a purely geometrical one and is insensitive to the chemistry. However, it is indeed a function of the nucleus density. Two additional lines, given in Figure 4(a), show that the increase in the nucleus density gives rise to a decrease in the critical grain size.

Apparently, the density of the pre-existing nuclei varies with the steel grade and processing history. With respect to TRIP steels, the retained austenite may have experienced various thermal processings, and, therefore, the nucleus density in the retained austenite is probably higher than 10^{13} m^{-3}. If the diameter of a nucleus (oblate spheroid) is taken to be 20 nm and its half-thickness to be 1.2 nm,[35,45] the volume fraction of the potent nucleus is calculated to be $1.9 \cdot 10^{-7}$. It seems that there is no problem with respect to the requirement for the volume fraction of the potent nuclei.

Figure 4(b) shows the decrease of the critical grain size as a function of the increase of the nucleus density. It indicates that a critical grain size of 1 μm requires a nucleus density of $2.5 \cdot 10^{17}$ m^{-3} at an aspect ratio of 0.05.[37] This density is four orders larger than reported.[14] However, Haidemenopoulos *et al.*[23] mentioned that the total number of nucleation sites of all potencies may be as large as $2 \cdot 10^{17}$ m^{-3}, by quoting the results regarding Fe-Ni crystals.[24]

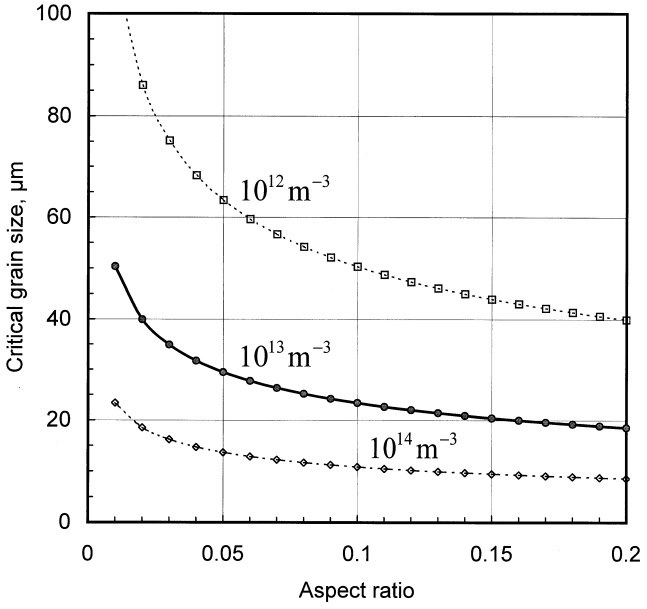

(*a*)

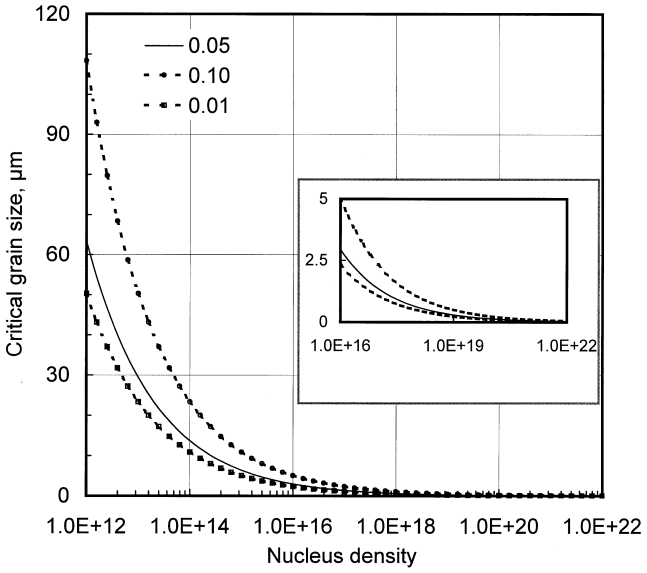

(*b*)

Fig. 4—Critical grain size of austenite particles as functions of (*a*) aspect ratio (three lines correspond to three different densities) and (*b*) nucleus density (three lines correspond to three different aspect ratios).

For the martensite reaction to become an athermal process, a sufficient number of nuclei should be available in the dispersed metastable austenite grains, some of which may be introduced by the applied stress, since it may modify the effective potency distribution of the pre-existing nucleation sites. It has been reported that the elastic interaction of dislocations (the potential heterogeneous martensitic nuclei) with internal stress concentrations may give rise to an increase in the nucleus density.[49] Practically, the martensite reaction has been observed to occur in fine austenite grains with a size magnitude of 1 μm. This means that whether the consumption of the pre-existing nuclei is responsible for the martensitic reaction kinetics depends on the actual nucleus density available in the system. The experimental

determination of the density is, therefore, important but very difficult.

B. *Problem on the Potent Embryos for Heterogeneous Nucleation*

If there are not sufficient heterogeneous nuclei, thermally activated nucleation is necessary. There are two types of nucleation: homogeneous and heterogeneous. Homogeneous nucleation was excluded based on Cohen's arguments, since the activation required is calculated to be as high as $3 \cdot 10^5 kT$.[45] Therefore, some form of heterogeneous nucleation must be postulated. It has been assumed that the transformation might begin spontaneously from suitable lattice defects, which serve as embryos and develop quickly into critical nuclei upon cooling or at the M_s temperature.[45] The problem remains, since subdividing the parent phase could also cause some of the small grains to be free from the suitable defects, *i.e.*, potent heterogeneous embryos.

If the martensite reaction in the dispersed austenite in the TRIP steels is athermal, thermally activated nucleation is not allowed. However, a larger embryo density may be introduced by the dissociation of dislocations.[49] Yet, it is still questionable whether such a large density of defects required is available in the dispersed austenite. Thus, it is worthwhile to calculate how many potent embryos or nuclei can be introduced by an applying stress and to check if a homogeneous (thermally activated) nucleation mechanism can be applied to the martensitic transformation.

C. *Chemical Stabilization*

The chemical stabilization is very clear, since the decomposition of austenite prior to the martensite reaction gives rise to the enrichment of carbon in the retained austenite, as shown in Figure 2(b). The chemical stabilization could be easily estimated if the influence of the carbon concentration on the M_s temperature were known. As collected in our previous article,[25] there are many empirical equations[25,50–52] describing the influence of carbon on the M_s temperature.[50,51,53] In Figure 5, experimental continuous cooling transformation (CCT) or time-temperature transformation (TTT) diagrams of 57 engineering steels (those containing a high carbon concentration and low alloying elements) have been chosen, and the influence of alloying elements other than that of C has been mathematically subtracted.[25] The choice of both CCT and TTT diagrams is based on the fact that M_s is insensitive to cooling rate up to 50,000 °C/s.[54,55] The data points shown in this figure virtually represent the influence of C on the M_s temperature. Two straight lines show the linear dependence of M_s on the carbon concentration by taking different coefficients. It is clear that the linear relationship works very well within the carbon concentration range from 0.2 and 0.8 mass pct. However, when the carbon concentration is larger than 1.2 mass pct, the use of the same linear equation will introduce large error. By examining the data points shown in Figure 5, we introduce an exponential dependency equation:

$$M_s\,(\mathrm{K}) = 273 + 545.8 \cdot e^{-1.362 w_C} \qquad [14]$$

where w_C represents the mass percentage of carbon in the steel. The previous equation describes the decrease of the

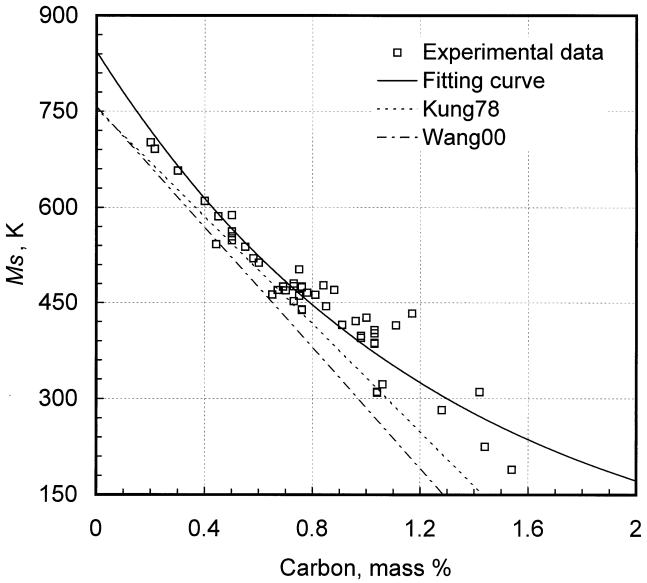

Fig. 5—Dependence of the M_s temperature on the carbon concentration in an Fe-C-1.5Si-1.5Mn steel; data points are chosen from collections listed in our previous publication.[30]

M_s temperature accompanying the increase in the carbon concentration in the Fe-C-1.5Mn-1.5Si model alloy, which corresponds to the retained austenite in the Fe-0.2C-1.5Mn-1.5Si TRIP steel. Note that in contrast to all previous empirical equations[25,50–52] describing the influence of carbon on the M_s temperature,[50,51,53] we choose an exponential expression so that the influence of carbon is toned down at high carbon concentrations. The use of a nonlinear equation is theoretically reasonable, since both the substructure and the habit planes of the martensite change with the increase of carbon concentration. What is interesting is that the constant obtained here approximately equals other equations, although the fitting methods are quite different. Equation [14] shows that, at a carbon level of 2 mass pct, the M_s temperature is reduced to 308 K. With respect to the retained austenite in TRIP steels, whose carbon concentration ranges from 1.0 to 2.0 mass pct, the M_s temperature should be between 473 °C and 308 °C, which is higher than room temperature. Thus, a certain amount of retained austenite would transform into martensite if no other stabilization mechanism were available.

D. *Relation between* M_s *and Critical Driving Force*

If the martensite transformation is intrinsically a plastic deformation requiring the shift of the whole interface, the barrier to this movement is called frictional work,[56,57] which is enhanced by the solid-solution strengthening of alloying elements. In such an approach, the following parameters should be taken into account: the Zener ordering of carbon atoms, the internal-defect energy of martensite, the interfacial energy, the elastic strain energy, and the fault energy serving as a driving force for the athermal nucleation. Following the classical expression,[16,58,59] the total energy change attending the formation of 1 mole of martensite is rewritten here as[25]

$$\Delta G_m^{\gamma\to\alpha} = (G_m^{\gamma} - G_m^{\alpha}) - (E_m^{\eta} + E_m^{D}) + (E_m^{e} + E_{\perp}^{\alpha'} + \text{Ɇ}_m) = \Delta G_{Ch}^{m} - \mathrm{E}_m^{\text{extra}} + \mathrm{E}_m^{\text{barrier}} \quad [15]$$

The first term on the right-hand side of the previous equation, ΔG_{Ch}^{m}, is the chemical driving force,[16] or the molar Gibbs free-energy difference between austenite and ferrite with the same composition (athermal transformation), which also includes the accompanying magnetic energy change. The value of ΔG_{ch}^{m} can be calculated directly by any thermodynamic database software package, such as MTData, by assuming that the martensitic ferrite and the austenite have the same chemical composition.[26] This means neither substitutional alloying atoms nor interstitial atoms are allowed to diffuse during the martensite formation. The method to calculate this energy term has been described elsewhere.[21] For the Fe-C-1.5Si-1.5Mn alloys, calculated thermodynamic results by MTData are presented in Figure 6(a), where different curves correspond to different carbon concentrations ranging from 1.0 to 2.0 mass pct. The practical M_s temperature of the retained austenite must be around or below room temperature; otherwise, it could not remain metastable at room temperature.[15] However, the heat capacities of phases listed in most of the thermodynamic databases are valid only above ambient temperature. To deal with this, we first calculated the critical driving forces at temperatures above 298 K, then regressed them to obtain an equation. We chose a polynomial expression for the temperature dependence of the chemical driving energy as

$$-\Delta G_m^{\gamma\to\alpha} = a_6 \cdot T^6 + a_5 \cdot T^5 + a_4 \cdot T^4 + a_3 \cdot T^3 + a_2 \cdot T^2 + a_1 \cdot T^1 + a_0 \quad [16]$$

The constants in Eq. [16] have been determined and are used hereafter to calculate the chemical driving force. The units of the critical driving force and temperature are given in J/mole and Kelvin, and the base alloy composition is Fe-C-1.5Mn-1.5Si (mass pct).

Note that the chemical driving force calculated by the previous equation does not consider the influence of the austenite grain boundary, which brings about extra energy (grain-boundary energy). Fortunately, the grain-boundary structure of austenite does not change much after the martensite transformation, since the formation of a martensite does not consume the area of the original austenite grain boundary.

The second term, $-E_m^{\text{extra}}$, is actually the extra driving force for the martensite transformation. The term E_m^{η} is the energy arising from the spontaneous ordering of carbon atoms at the M_s temperature, *i.e.*, the Zener ordering energy.[59,60] It depends largely on the M_s temperature and the carbon concentration in the steel. It can be calculated separately by the Zener–Fisher model.[59] The substitutional alloying elements also exert a certain influence on the Zener ordering energy by slightly changing the lattice parameters of austenite and martensite. By considering the temperature and chemistry dependencies of the elastic modulus and lattice parameters, we can calculate the Zener ordering energy[21] accompanying the reactions in this steel. An example of the calculated result is shown in Figure 6(b).

The term E_m^{D} is the fault energy, which is very important for the heterogeneous nucleation theory of martensite and serves as an extra driving force. This is normally assumed to be independent of the steel chemistry and temperature.[49,61]

The third term, E_m^{barrier}, is the transformation barrier. The term E_m^{e} is the elastic transformation strain energy arising from lattice deformation, which includes both homogeneous and heterogeneous deformation. Only homogeneous deformation produces a macroscopic shape (namely, surface relief) effect. Furthermore, a homogeneous deformation is composed of a shear component parallel to the invariant plane-strain (IPS) plane, which stays neither distorted nor rotated, and a dilatational component perpendicular to the IPS plane. The elastic energy is not only a function of the mole fraction of the precipitate and the composition of the matrix, since both elastic constants and lattice parameters are functions of composition, but also function of the phase morphology, *i.e.*, the shape (aspect ratio) and distribution of the martensitic phase[62] and, of course, the transformation temperature. Based on the simple Bain model, both of them depend only on the lattice parameters of the matrix and product.[63,64] Figure 6(c) shows an example of the calculated elastic energy accompanying the formation of 1 mole of martensite at room temperature in the Fe-C-1.5Mn-1.5Si steels. It is, of course, an improper assumption, since the M_s temperature in question is not equal to room temperature; but it indeed shows the influence of carbon on the elastic energy by changing the lattice parameters and elastic moduli. What is seen in Figure 6(c) is obviously inconsistent with the idea that the role of carbon in suppressing the martensite reaction arises from its raising the elastic energy.[65] Instead, it is reasonable to attribute its effect to its reducing the chemical driving force (Figure 6(a)).

The second part of the third term in Eq. [15], $E_{\perp}^{\alpha'}$, is the internal defect energy stored in the as-formed martensite phase, which is determined only by the defect density of the martensite plates when the volume fraction of the martensite is given. The defect density of the martensite structure formed in the retained austenite in the TRIP steels is not expected to be very sensitive to the length scale of the martensite plates or the narrow reaction-temperature range (for the martensite reaction in the retained austenite, the temperature range is just around room temperature). Therefore, similar to the term W_f^*, which will be discussed later, the term associated with the internal defect energy will be automatically incorporated into the fitting parameters in Eq. [20].

The last part of the third term is Ɇ_m, the interfacial energy, which is the important item needed to be discussed in this study, since most of the other types of energy mentioned previously are hardly influenced by the austenite grain size. The interfacial energy associated with the formation of 1 mole of martensite under the situation described previously is

$$\text{Ɇ}_m = A_0^{\alpha'}\, n_m^{\alpha'} \gamma_{\alpha'/\gamma} = \frac{2V_m^{\alpha'}\gamma_{\alpha'/\gamma}}{\delta} = \frac{2V_m^{\alpha'}\gamma_{\alpha'/\gamma}}{\imath d_0} \quad [17]$$

where $\gamma_{\alpha'/\gamma}$ is the specific surface energy of the martensite/austenite interface.

At the M_s temperature, Eq. [15] becomes

$$0 \geq (G_m^{\gamma} - G_m^{\alpha})^* - (E_{\eta}^* + E_{D}^*) + (E_e^* + E_{\perp}^* + \text{Ɇ}_m^*) + W_f^* \quad [18]$$

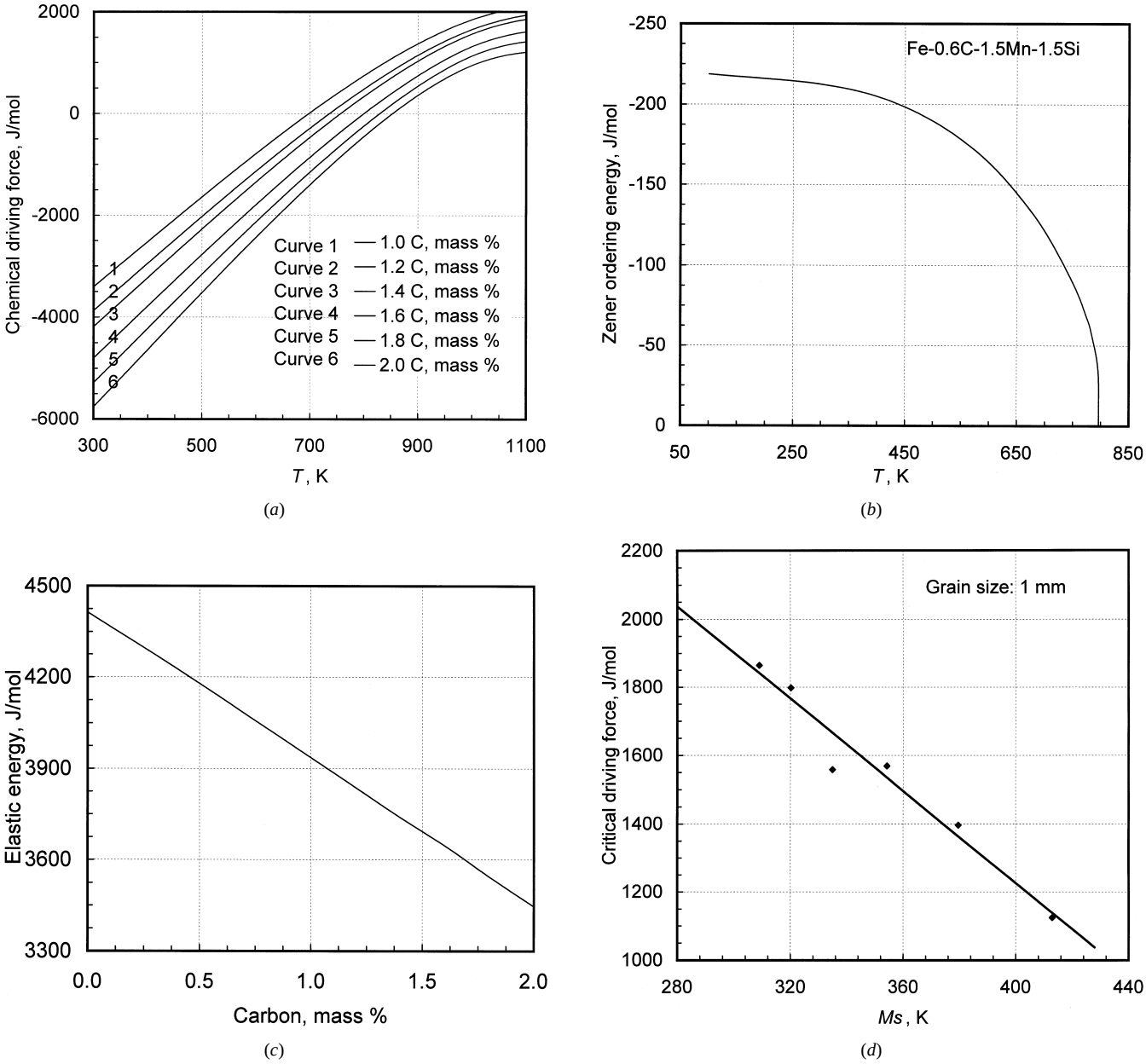

Fig. 6—Gibbs free energy change accompanying the formation of 1 mole martensite from austenite; (*a*) Gibbs energy difference between austenite and martensite as a function of temperature; (*b*) magnitude of Zener ordering energy accompanying the possible martensitic decomposition in the Fe-0.6C-1.5Mn-1.5Si steel; (*c*) elastic energy including both dilatational and shear components (their corresponding strains are determined based on the simple Bain model); and (*d*) net energy change in the system by adding the chemical driving force, the Zener ordering energy, and the elastic energy as a function of the M_s temperature

where W_f^* is all other types of energy, which may exist but cannot be properly considered. Following our previous analysis,[30,21] we move our predictable items in Eq. [18] to the right-hand side, assume that the remaining part is a function of M_s, and rewrite Eq. [18] as

$$-(G_m^{\gamma} - G_m^{\alpha})^* + E_{\eta}^* - E_e^* - \cancel{E_m^*} = W_f^* - E_D^* = g(M_s) - \cancel{E_m^*} = f(M_s) \quad [19]$$

For the test alloy, the left-hand side of the previous equation can be calculated. It is plotted against M_s in Figure 6(d). The function $f(M_s)$ can be approximately given by

$$E_{\text{net}}\ (\text{J/mole}) = f(M_s) = A + B \cdot M_s = 3931 - 6.761\ M_s(\text{K}) \quad [20]$$

It is clear that the coefficients in Eq. [20] depend on what are included in the energy item, $f(M_s)$. The removal or introduction of any types of energies will give rise to a change in the coefficients. If the grain-size effect on the interfacial energy increase is negligible, at the temperature of M_s, $g(M_s) = f(M_s)$, otherwise, $g(M_s) \neq f(M_s)$.

Equation [20] is very important, since it relates the energy change of the system to the M_s temperature. Using this

equation, we can easily estimate the effect of the interfacial energy, applied strain, internal stored energy, *etc.*, on the M_s temperature of a steel. A similar method has been previously applied to relate the critical driving force to the M_s temperature. In the next section, this equation will be used to determine the influence of an interfacial energy change due to a grain-size reduction on the M_s temperature.

E. *Stabilization Due to Increase in Interfacial Energy*

Grain boundaries generally serve to stabilize the parent phase, since the growth of martensite stops at a grain boundary.[66] It is clear in Eq. [17] that the total interfacial energy is directly related to the thickness of the martensite plates or, indirectly, to ι and d_0. This also means that the decrease in the austenite grain size requires an increase in the transformation driving force, correspondingly leading to a decrease in the M_s temperature. Figure 7(a) illustrates the change of the total interfacial energy, attending the formation of 1 mole of martensite plates at the M_s temperature, with the decrease of the austenite grain size at three specific aspect ratios of 0.05, 0.1, and 0.01. The interface is assumed to be semicoherent, with an average specific energy of 0.15 J/m^2 based on the calculation for the dislocation model of the interface.[31,45] From the zoomed-in part of Figure 7(a), it is concluded that the variation in the total interfacial energy is indeed negligible when the grain size is larger than 10 μm. As was pointed out earlier, the grain size of engineering steels is between 20 and 100 μm. This means that the influence of the austenite grain size on the M_s temperature of general engineering steels can be ignored. However, it is also clear in Figure 7(a) that when the grain size falls between 0.1 and 10 μm, the influence changes exponentially and depends on the aspect ratio. The lower the aspect ratio, the more significant the influence.

If potent embryos or nuclei (either thermally activated or pre-existing heterogeneously) are available for the martensitic reaction, the interfacial energy will be the most important parameter to decrease the M_s temperature. Rewriting Eq. [19] by substituting Eq. [17] and [20], we obtain the critical thickness of the martensite plate in the general form

$$\delta^* = \frac{2V_m^{\alpha'}\gamma_{\alpha/\gamma}}{f(M_s) + E_m^* - (A + B \cdot M_s)} \qquad [21]$$

If the aspect ratio is a constant for a certain alloy, Eq. [21] can be rewritten in the form

$$d_0^* = \frac{2\iota V_m^{\alpha'}\gamma_{\alpha/\gamma}}{f(M_s) + E_m^* - (A + B \cdot M_s)} \qquad [22]$$

Apparently, if the austenite grain size is less than d_0^*, no martensite transformation occurs in the steel.

Equation [22] is a general description of the influence of the austenite grain size on the M_s temperature. Most of the parameters involved in the equation are actually dependent on the steel chemistry. As generalized in our previous article,[21] the parameters A and B depend on the alloy system. Let us examine the numerical effect of the grain size on the M_s temperature in small austenite particles. For a given carbon concentration, the M_s temperature can be estimated by using Eq. [14]. Then, the critical chemical driving force for the martensitic reaction in the bulk alloy (ΔG_{ch}^*) can be obtained from Figure 6(a) or Eq. [16]. All other types of

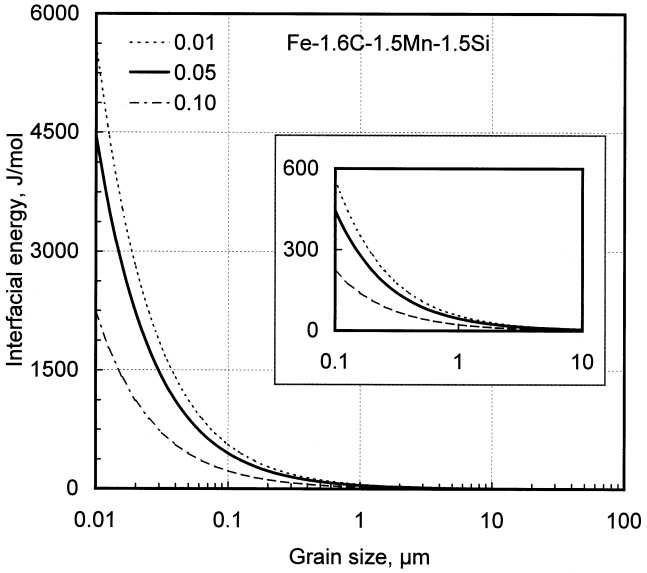

(*a*)

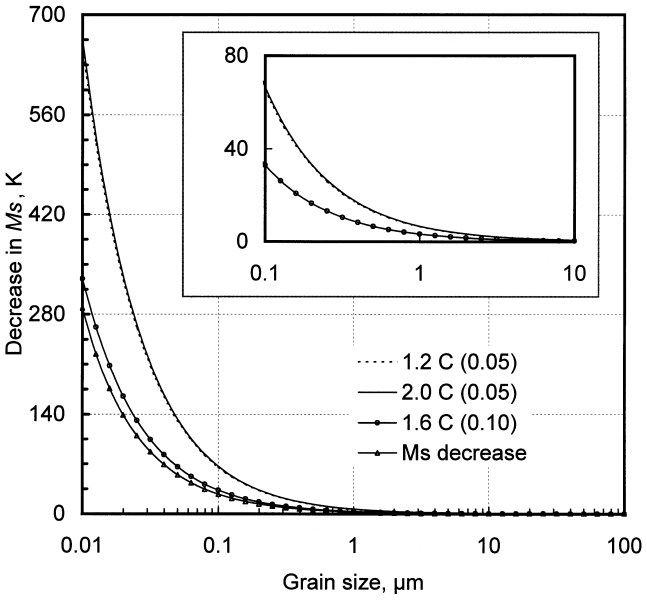

(*b*)

Fig. 7—Stabilization of retained austenite due to grain size effect. (*a*) Total interfacial energy accompanying the formation of one mole martensite at the M_s temperature as a function of the retained austenite grain size; the unit interfacial energy is taken as 0.15 J/m^{-2}, and the three lines correspond to different aspect ratios. (*b*) Decrease in M_s temperature due to the decrease of austenite grain size (for details about the four curves, refer to the text).

energy can be calculated following a similar way, shown in Figure 6. Combining Eqs. [19] and [20] gives rise to

$$g(T) = A + B \cdot M_s + E_m^* \qquad [23]$$

The solution to Eq. [23] is the M_s temperature of small austenite particles. If the temperature dependence of g is neglected, the decrease of the M_s temperature due to the grain-size effect is given by

$$\Delta M_s = \left|\Delta E_m^*/B\right| \qquad [24]$$

as shown Figure 7(b). Two of the curves have the same aspect ratio of 0.05, but with different carbon concentrations

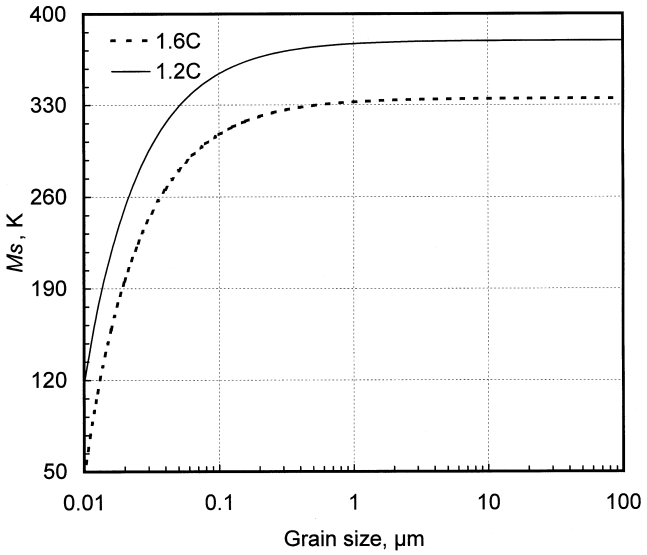

Fig. 8—M_s temperatures of the retained austenite with carbon concentrations equal to 1.2 and 1.6 mass pct as a function of the grain size.

of 1.2 and 2.0 mass pct. The other curve corresponds to an aspect ratio of 0.10 and a carbon concentration of 1.6 mass pct. It seems that the influence is hardly dependent on the carbon concentration, but indeed varies exponentially with the grain size and aspect ratio. Note that the M_s temperature is determined by balancing the system energies, as listed in Eq. [19].[21] When the M_s temperature is changed from M_s to $M_s + \Delta M_s$, all the energy terms, such as the Gibbs energy, elastic energy, and Zener ordering energy, have been changed, since all of them are temperature dependent. However, taking the first-order approximation, we ignore the changes within the temperature range of ΔM_s in Eq. [24]. If the temperature dependencies of various types of energies have been taken into account properly, the decrease of M_s with decreasing grain size can also be determined. For an alloy containing 1.6 mass pct C with an aspect ratio of 0.05, the change of M_s against grain size was calculated and is shown in Figure 7(b) by the curve with triangular data points. Note that the decreased amount of the M_s is reduced.

In addition to the decrease, the M_s temperature itself of austenite particles can be calculated by solving Eq. [23]. Figure 8 shows the M_s temperature of retained austenite with carbon concentrations equaling 1.2 and 1.6 mass pct. This figure shows again that the influence of austenite grain size becomes significant when the grain size is down to 0.1 μm. In fact, when the retained austenite particles are larger than 1 μm, they are relatively unstable and transform to martensite at a smaller applied strain and, thus, will not contribute much to the ductility of the material, as was investigated by other authors.[17] Extremely small austenite particles of a size smaller than 0.02 μm are also useless for the TRIP effect, since the M_s temperature of the retained austenite is so reduced that no strain-induced martensitic transformation occurs.

VI. SUMMARY

Theoretical analysis indicates that various stabilization mechanisms may operate during the decomposition of retained austenite in the TRIP steels. The results can be summarized as follows.

1. Whether an athermal nucleation mechanism operates in the course of the martensitic decomposition of the dispersed metastable austenite depends on the potential nucleus density and the austenite grain. If the austenite grain size is around 1 μm, theoretical calculation indicates that a nucleus density as large as $2.5 \cdot 10^{17}$ m^{-3} is required for an athermal nucleation kinetics. If the required nucleus density cannot be satisfied, the shortage of nuclei may be responsible for the austenite retention. The aforementioned conclusion has been made providing that burst transformation does not dominate the formation mechanism of martensite.
2. Chemical stabilization due to the enrichment of carbon in the retained austenite is the most important operational mechanism. The M_s temperature of Fe-C-1.5Mn-1.5Si is reduced to a range from 473 to 308 K when the carbon enriched in austenite increases from 1.0 to 2.0 mass pct. The M_s temperature of the alloy is exponentially related to the carbon concentration of retained austenite by the equation of M_s (K) $= 273 + 545.8 \cdot e^{-1.362 w_C}$.
3. The chemical driving force, elastic energy, and Zener ordering energy associated with the formation of 1 mole of martensite in the austenite with different grain sizes have been calculated. A function describing the M_s temperature and the energy change of the system has been found.
4. The influence of the grain size on the M_s temperature has been estimated by considering the introduction of extra interfacial energy upon the formation of 1 mole of martensite. It is pointed out that the decrease in the austenite grain size gives rise to a significant decrease in the M_s temperature. A retained austenite with a grain size smaller than 0.01 μm is useless for TRIP steels, since it will not transform to martensite, while that with a grain size larger than 1 μm may be equally useless, since it will immediately transform to martensite upon cooling or during application of small stress.

Appendix

Let us consider a 1-mole (lattice-site) system. After intercritical annealing and isothermal holding, three phases (ferrite, bainite, and retained austenite) exist in the system, with the mole fractions of X_P, where P denotes the three phases. By definition,

$$\sum_P X_P = 1 \qquad [A1]$$

If the average carbon concentration of the mass alloy is x_γ^0 (mole atom fraction), the total mole number of carbon atoms in the system is calculated as

$$n_C = \frac{x_\gamma^0}{1 - x_\gamma^0} \qquad [A2]$$

It is easy to write the mole number of carbon atoms in each phase as follows:

$$n_C^P = \frac{X_P x_P}{1 - x_P} \qquad [A3]$$

where x_P represents the carbon mole fractions of the corresponding phases. To equilibrate the summation of Eq. [A3] over P with Eq. [A2] generates

$$\sum_P \frac{X_P x_P}{1 - x_P} = \frac{x_\gamma^0}{1 - x_\gamma^0} \quad [A4]$$

The function of the carbon content in the retained austenite is obtained by rewriting Eq. [A4]:

$$x_\gamma = \left[1 + \frac{X_\gamma}{\dfrac{x_\gamma^0}{1 - x_\gamma^0} - \dfrac{X_B x_B}{1 - x_B} - \dfrac{X_F x_F}{1 - x_F}} \right]^{-1} \quad [A5]$$

where the indices of B and F represent bainite and ferrite, respectively. Meanwhile, the volume fraction of a phase P is related to its mole fraction by

$$f_P = \frac{X_P V_P^m}{\sum_Q X_Q V_Q^m} \quad [A6]$$

where V_P^m is the molar volume of the P phase, which can be calculated from the lattice constants, and the summation of Q is over three phases. It is easy to write

$$\sum_P f_P = 1 \quad [A7]$$

Combining Eq. [A5] through [A7], we obtain the relation between the mole fraction of carbon atoms and the volume fraction of the retained austenite:

$$x_\gamma = \left[1 + \frac{X_B V_B^m + X_F V_F^m}{\dfrac{x_\gamma^0}{1 - x_\gamma^0} - \dfrac{X_B x_B}{1 - x_B} - \dfrac{X_F x_F}{1 - x_F}} \frac{f_\gamma}{V_\gamma^m (1 - f_\gamma)} \right]^{-1} \quad [A8]$$

Note that there are nine variables of x_P, X_P, and f_P, but only three equations ([A1], [A6], and [A7]) are available. However, if the carbon concentrations of bainite and ferrite are assumed to be the same and are taken to be the same equilibrium carbon concentration as that in the ferrite, then the only parameter needed to solve Eq. [A8] is either X_B or X_F.

REFERENCES

1. A. Zarei Hanzaki and S. Yue: *Iron Steel Inst. Jpn. Int.*, 1997, vol. 37, pp. 583-89.
2. A. Zarei Hanzaki, P.D. Hodgson, and S. Yue: *Iron Steel Inst. Jpn. Int.*, 1995, vol. 35, pp. 79-85.
3. J. Wang and S. van der Zwaag: Report No. P00.5.044, Netherlands Institute for Metals Research, Delft, 2000, pp. 1-21.
4. W. Bleck, J. Ohlert, and K. Papamantellos: *Steel Res.*, 1999, vol. 70, pp. 472-97.
5. J. Wang and S. van der Zwaag: *ECSC Steel Workshop on Advanced Hot Rolling Practice and Products*, Düsseldorf, Oct. 2000.
6. V.F. Zackay, D. Parker, D. Fahr, and R. Bush: *Trans. ASM*, 1967, vol. 60, pp. 252-59.
7. J.R. Bradley, H.I. Aaronson, K.C. Russel, and W.C. Johnson: *Metall. Trans. A*, 1977, vol. 8A, pp. 1955-61.
8. S. Yamamoto, H. Yokoyama, K. Yamada, and M. Niikura: *Iron Steel Inst. Jpn. Int.*, 1995, vol. 35, pp. 1020-6.
9. S. Kajiwara, S. Ohno, and K. Honma: *Phil. Mag. A*, 1991, vol. 63, pp. 625-44.
10. M.R. Meyerson and S.J. Rosenburg: *Trans. ASM*, 1954, vol. 56, pp. 1225-50.
11. M.G.H. Wells: *J. Iron Steel Inst.*, 1961, vol. 198, pp. 173-74.
12. A.R. Entwisle: *Metall. Trans.*, 1971, vol. 2, pp. 2395-2407.
13. C.L. Magee: *Metall. Trans.*, 1971, vol. 2, pp. 2419-30.
14. R.E. Cech and D. Turnbull: *Trans. AIME*, 1956, vol. 206, pp. 124-32.
15. A. Zarei Hanzaki, P.D. Hodgson, and S. Yue: *Metall. Mater. Trans. A*, 1997, vol. 28A, pp. 2405-14.
16. J.C. Fisher, J.H. Hollomon, and D. Turnbull: *Trans. AIME*, 1949, vol. 185, pp. 691-700.
17. D.Q. Bai, A. Di Chiro, and S. Yue: *Mater. Sci. Forum*, 1998, vols. 284–286, pp. 253-60.
18. W.J. Botta, D. Negri, and A.R. Yavari: *Mater. Sci. Forum*, 1999, vols. 312–314, pp. 387-92.
19. M. Hillert and J. Ågren: *Advances in Phase Transitions*, J.D. Embury and G.R. Purdy, Oxford, United Kingdom, 1988, pp. 1-19.
20. J.R. Bradley and H.I. Aaronson: *Metall. Trans. A*, 1981, vol. 12A, pp. 1729-41.
21. J. Wang, P.J. van der Wolk, and S. van der Zwaag: *Mater. Trans. JIM*, 2000, vol. 41, pp. 769-76.
22. J. Wang and S. van der Zwaag: unpublished research.
23. G.N. Haidemenopoulos, M. Grujicic, G.B. Olson, and M. Cohen: *J. Alloys Compounds*, 1995, vol. 220, pp. 142-47.
24. L. Kaufman and M. Cohen: *Trans. AIME*, 1956, vol. 206, pp. 1393-1401.
25. J. Wang, P.J. van der Wolk, and S. van der Zwaag: *Mater. Trans. JIM*, 2000, vol. 41, pp. 761-68.
26. R.H. Davies, A.T. Dinsdale, J.A. Gisby, S.M. Hodson, and T.I. Barry: *MTData Handbook*, National Physical Laboratory, Middlesex, United Kingdom, 1994.
27. H.I. Aaronson, W.T.J. Reynolds, G.J. Shiflet, and G. Spanos: *Metall. Trans. A*, 1990, vol. 21A, pp. 1343-80.
28. H.C. Chen, H. Era, and M. Shimizu: *Metall. Trans. A*, 1989, vol. 20A, pp. 437-45.
29. J. Wang, H.S. Fang, Z.G. Yang, and Y.K. Zheng: *Iron Steel Inst. Jpn. Int.*, 1995, vol. 35, pp. 992-1000.
30. J. Wang, P.J. van der Wolk, and S. van der Zwaag: *J. Mater. Sci.*, 2000, vol. 35, pp. 4393-4404.
31. S. van der Zwaag: *Mater. Sci. Forum*, 1998, vols. 284–286, pp. 27-38.
32. J. Wang: *Lattice Parameters of Phases in Steels, Ver. 0.7.3*, Netherlands Institute for Metals Research, Delft, 2000.
33. E.O. Hall: *Proc. Phys. Soc. Ser.*, 1951, vol. B64, pp. 747-53.
34. N.J. Petch: *J. Iron Steel Inst.*, 1953, vol. 174, pp. 25-28.
35. L. Kaufman and M. Cohen: *Prog. J. Met. Phys.*, 1958, vol. 7, pp. 165-246.
36. X.Q. Zhao and Y.F. Han: *Metall. Mater. Trans. A*, 1999, vol. 30A, pp. 884-87.
37. A.K. Jena and M.C. Chaturvedi: *Phase Transformation in Materials*, A Simon & Schuster Company, NJ, 1992.
38. J.R.C. Guimaraes and J.C. Gomes: *Metall. Trans. A*, 1979, vol. 10A, pp. 109-12.
39. R. Datta and V. Raghavan: *Mater. Sci. Eng.*, 1982, vol. 55, pp. 239-46.
40. G. Ghosh and V. Raghavan: *Mater. Sci. Eng.*, 1986, vol. 79, pp. 223-31.
41. V. Raghavan: in *Martensite: a Tribute to Morris Cohen*, G.B. Olson, W.S. Owen, and M. Cohen, eds., ASM, Metals Park, OH, 1992, pp. 197-225.
42. M. Grujicio and Y. Zhang: *J. Mater. Sci.*, 2000, vol. 35, pp. 4635-47.
43. W.Y.C. Chen and P.G. Winchell: *Metall. Trans. A*, 1976, vol. 7A, pp. 1177-82.
44. W.Y.C. Chen, E.N. Jones, and P.G. Winchell: *Metall. Trans. A*, 1978, vol. 9A, pp. 1659-61.
45. J.W. Christian: *Martensite: Fundamentals and Technology*, E.R. Petty, ed., Longman, London, 1970, pp. 11-42.
46. D. Turnbull and B. Vonnegut: *I & E Chem.*, 1952, vol. 44, p. 1292.
47. V. Raghavan and A.R. Entwisle: *Physical Properties of Martensite and Bainite*, ISI, London, 1965, pp. 29-37.
48. H.S. Fang, J. Wang, Z.G. Yang, C.M. Li, and Y.K. Zheng: *Metall. Mater. Trans. A*, 1996, vol. 27A, pp. 1533-43.
49. G.B. Olson and M. Cohen: *Metall. Trans. A*, 1976, vol. 7A, pp. 1897-1904.
50. K.W. Andrews: *J. Iron Steel Inst.*, 1965, vol. 203, pp. 721-27.
51. W. Steven and A.G. Haynes: *J. Iron Steel Inst.*, 1956, vol. 183, pp. 349-59.
52. C.Y. Kung and J.J. Rayment: *Metall. Trans. A*, 1982, vol. 13A, pp. 328-31.
53. P. Payson and H. Savage: *Trans. ASM*, 1944, vol. 33, pp. 261-80.

54. M.J. Bibby and J.G. Parr: *J. Iron Steel Inst.*, 1964, vol. 202, pp. 100-04.
55. A.B. Greninger: *Trans. ASM*, 1942, vol. 30, pp. 1-26.
56. G. Ghosh and G.B. Olson: *Acta Metall. Mater.*, 1994, vol. 42, pp. 3361-70.
57. G. Ghosh and G.B. Olson: *Acta Metall. Mater.*, 1994, vol. 42, pp. 3371-79.
58. J.C. Fisher, J.H. Hollomon, and D. Turnbull: *J. Appl. Phys.*, 1948, vol. 19, pp. 775-84.
59. J.C. Fisher: *Trans. AIME*, 1949, vol. 185, pp. 688-90.
60. C. Zener: *J. Appl. Phys.*, 1949, vol. 20, p. 950.
61. G.B. Olson and M. Cohen: *Metall. Trans. A*, 1976, vol. 7A, pp. 1915-23.
62. J.W. Cahn and F. Larch: *Acta Metall.*, 1984, vol. 32, pp. 1915-23.
63. J.S. Bowles and J.K. Mackenzie: *Acta Metall.*, 1954, vol. 2, pp. 127-37.
64. M.S. Wechsler, D.S. Lieberman, and T.A. Read: *Trans. AIME*, 1953, vol. 197, pp. 1503-15.
65. D.K. Felbeck and A.G. Atkins: *Strength and Fracture of Engineering Solids*, Prentice-Hall, Inc., Englewood Cliffs, NJ, 1984.
66. Z. Nishiyama: *Martensitic Transformation*, Academic Press, New York, NY, 1978.